Hydroinformatics'96, Müller (ed.) © 1996 Balkema, Rotterdam. ISBN 90 5410 852 5

Extension of the 2-dimensional shallow water approach using moment equations

Daniel R. Naef
Laboratory of Hydraulics, Hydrology and Glaciology (VAW), Swiss Federal Institute of Technology, Zürich, Switzerland

ABSTRACT: The 2d shallow water equations can be used only for cases where the vertical velocity is negligible and the hydrostatic pressure distribution is not violated. The presented method allows vertical velocities and introduces additional pressure terms. A further improvement is achieved for the depth averaged horizontal velocities, which are replaced by a linear distribution. The derivation of the additional equations is outlined and some examples are given.

1 INTRODUCTION

The 2-dimensional shallow water equations are not applicable for cases where the vertical velocity can not be neglected and the hydrostatic pressure distribution assumption is too stringent. A new method, the depth averaged and momentum equations, as derived by Steffler & Jin (1993) for the 1-dimensional case, is extended to 2 dimensions and for practical purpose somewhat simplified. First numerical examples for the 1d case are presented by Khan & Steffler (1996). The new approach allows computations where vertical velocities play an important role, without extending to the full 3d Navier-Stokes equations with free surface. Compared to a 3d calculation the number of elements therefore can be kept relatively small, and an additional nonlinearity caused by the free surface does not occur.

However the new approach increases the number of unknowns from 3 to 10 compared to the classical shallow water equations and therefore needs reasonable computer resources. Resolution of further flow details is achieved by introducing these additional unknowns.

2 VERTICALLY AVERAGED EQUATIONS

The depth-averaged equations are based on the fundamental assumption of a hydrostatic pressure distribution.

In addition to the 3 shallow water equations, extended with the terms for the additional unknowns, new equations have to be considered, since the number of variables increases. The bed and surface kinematic conditions form two of these equations. The vertical momentum is another equation to be introduced. Finally, the moment of the continuity and of the three momentum equations are formulated. They can be derived by vertically averaging the Reynolds equations after multiplying through by the vertical coordinate z and subtracting the mean elevation times the vertically averaged equations. This derivation corresponds to the first moment about the mid-depth point. The 10 independent equations are solved with the FEM using a toolbox developed by P. Rutschmann (1994).

Instead of one depth averaged velocity for each horizontal direction, a linear distribution is assumed and therefore 2 additional unknowns are introduced. The hydrostatic pressure distribution assumption of the classical shallow water equations is no longer applied. An excess bottom pressure and a mid-depth pressure factor allow the simulation of a quadratic pressure distribution over the water depth in addition to the hydrostatic pressure. For the vertical velocities a quadratic formulation is implemented, using the bottom and the surface vertical velocities as unknowns, as well as an additional quadratic factor describing the mid-depth unlinearity.

The definition of the parameters is given in Figure 1, the x-y direction forming the horizontal frame with the corresponding velocities u, resp. v. The vertical direction z with the velocity w and the indices h for values at the surface, resp. b for the bottom. σ and τ indicating normal and shear stresses respectively. The mean value of $\bar{z}$ is defined as:

$$\bar{z} = z_b + \frac{h}{2} \tag{1}$$

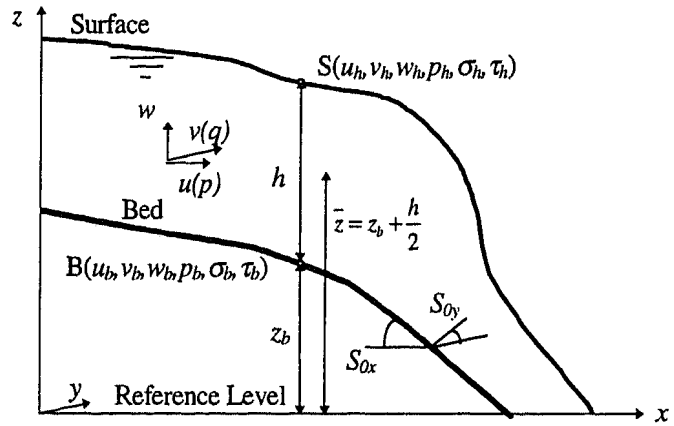

Figure 1: Definition sketch.

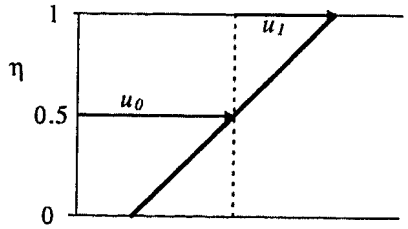

Figure 2: Horizontal Velocity Distribution.

The basic assumption of the method are described in the following section. Instead of using the depth averaged velocity, a linear, zero mean distribution, as shown in Figure 2, is assumed for the two horizontal velocities. The velocity u is given by the depth averaged value u_0, and an excess velocity u_1 at the surface.

$$u = u_0 + u_1(2\eta - 1) \tag{2}$$

where the nondimensional vertical coordinate η is defined by $\eta = \frac{z - z_b}{h}$ (3)

For the y direction the same type of horizontal velocity distribution is assumed, introducing the mean value v_0 and the velocity difference, from the mean value, at the surface v_1:

$$v = v_0 + v_1(2\eta - 1) \tag{4}$$

Although this linear distribution is an improvement compared with the depth averaged equation, a slip velocity at the bed is still allowed. There could be more accurate methods to dissolve the horizontal velocity terms, but the improvement is not found in a detailed resolution within the thin boundary layer, but in the overall behavior.

The vertical velocity distribution w is approximated by a quadratic variation. The kinematic conditions at the bed and the surface in addition to the moment of continuity equation provide the essential informations:

$$w = w_b(1 - \eta) + w_2 4\eta(1 - \eta) + w_h\eta \tag{5}$$

Figure 3 shows a plot of the vertical velocity

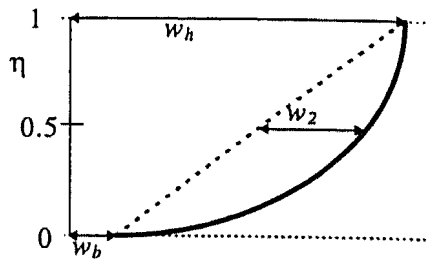

Figure 3: Vertical Velocity Distribution.

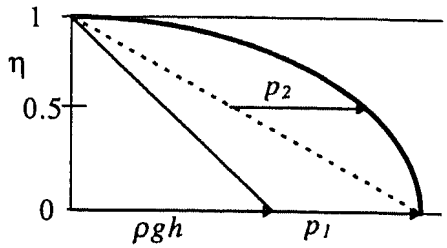

Figure 4: Pressure Distribution.

distribution. w_b and w_h indicate the vertical velocities at the bottom, resp. at the surface, whereas w_2 is the vertical velocity at the mid depth in excess to the average of w_b and w_h.

The final equations are formed in terms of the mean vertical velocity $\overline{w}$ instead of w_2, since the depth averaging process results in depth averaged values.

The quadratic pressure distribution, as shown in Figure 4, is formed of a linear pressure parameter p_1 at the bed, in excess to the hydrostatic pressure distribution, and a quadratic mid depth fraction p_2. g is the gravitational factor and ρ the density of the water.

$$p = (\rho gh + p_1)(1 - \eta) + p_2 4\eta(1 - \eta) \tag{6}$$

The kinematic boundary condition at the bottom is easy to fulfill, because the bottom is assumed to be rigid:

$$(u_0 - u_1)\frac{\partial z_b}{\partial x} + (v_0 - v_1)\frac{\partial z_b}{\partial y} - w_b = 0 \tag{7}$$

The kinematic boundary condition at the surface is described by the fact, that the flow through the surface is zero. Applying the velocity definitions given in equations (2) and (4), results in the following equation:

$$\frac{\partial h}{\partial t} + (u_0 + u_1)\left(\frac{\partial h}{\partial x} + \frac{\partial z_b}{\partial x}\right) + (v_0 + v_1)\left(\frac{\partial h}{\partial y} + \frac{\partial z_b}{\partial y}\right) - w_h = 0 \tag{8}$$

Starting with the Reynolds equations (Mass, x-, y- and z-Momentum)

$$\frac{\partial u}{\partial x} + \frac{\partial v}{\partial y} + \frac{\partial w}{\partial z} = 0 \tag{9}$$

$$\frac{\partial u}{\partial t}+\frac{\partial u^2}{\partial x}+\frac{\partial uv}{\partial y}+\frac{\partial uw}{\partial z}= \tag{10}$$
$$-\frac{1}{\rho}\frac{\partial p}{\partial x}+\frac{1}{\rho}\left(\frac{\partial \sigma_x}{\partial x}+\frac{\partial \tau_{xy}}{\partial y}+\frac{\partial \tau_{xz}}{\partial z}\right)$$

$$\frac{\partial v}{\partial t}+\frac{\partial uv}{\partial x}+\frac{\partial v^2}{\partial y}+\frac{\partial vw}{\partial z}= \tag{11}$$
$$\frac{1}{\rho}\frac{\partial p}{\partial y}+\frac{1}{\rho}\left(\frac{\partial \tau_{yx}}{\partial x}+\frac{\partial \sigma_y}{\partial y}+\frac{\partial \tau_{yz}}{\partial z}\right)$$

$$\frac{\partial w}{\partial t}+\frac{\partial uw}{\partial x}+\frac{\partial vw}{\partial y}+\frac{\partial w^2}{\partial z}= \tag{12}$$
$$\frac{1}{\rho}\frac{\partial p}{\partial z}+\frac{1}{\rho}\left(\frac{\partial \tau_{zx}}{\partial x}+\frac{\partial \tau_{zy}}{\partial y}+\frac{\partial \sigma_z}{\partial z}\right)-g$$

Depth averaging the mass conservation equation 9, embedding the previously given definitions in equations (2) and (4), yields to:

$$\frac{\partial h}{\partial t}+\frac{\partial hu_0}{\partial x}+\frac{\partial hv_0}{\partial y}=0 \tag{13}$$

This continuity equation is similar to the one resulting out of the depth averaging process, since the zero mean distribution of u_1, resp. v_1 leads to unchanged expressions.

Depth averaging of the momentum equations results with the mean stress quantities of $\bar{\sigma}$ and $\bar{\tau}$ in the x, resp. y-momentum equation:

$$\frac{\partial hu_0}{\partial t}+\frac{\partial hu_0^2}{\partial x}+\frac{1}{3}\frac{\partial hu_1^2}{\partial x}+\frac{\partial hu_0v_0}{\partial y}+\frac{1}{3}\frac{\partial hu_1v_1}{\partial y}+gh\frac{\partial(h+z_b)}{\partial x}+ \tag{14}$$
$$\frac{1}{2\rho}\frac{\partial hp_1}{\partial x}+\frac{2}{3\rho}\frac{\partial hp_2}{\partial x}+\frac{p_1}{\rho}\frac{\partial z_b}{\partial x}-\frac{1}{\rho}\frac{\partial h\bar{\sigma}_x}{\partial x}-\frac{1}{\rho}\frac{\partial h\bar{\tau}_{xy}}{\partial y}+\frac{\tau_{bx}}{\rho}=0$$

$$\frac{\partial hv_0}{\partial t}+\frac{\partial hv_0^2}{\partial y}+\frac{1}{3}\frac{\partial hv_1^2}{\partial y}+\frac{\partial hu_0v_0}{\partial x}+\frac{1}{3}\frac{\partial hu_1v_1}{\partial x}+gh\frac{\partial(h+z_b)}{\partial y}+ \tag{15}$$
$$\frac{1}{2\rho}\frac{\partial hp_1}{\partial y}+\frac{2}{3\rho}\frac{\partial hp_2}{\partial y}+\frac{p_1}{\rho}\frac{\partial z_b}{\partial y}-\frac{1}{\rho}\frac{\partial h\bar{\sigma}_y}{\partial y}-\frac{1}{\rho}\frac{\partial h\bar{\tau}_{xy}}{\partial x}+\frac{\tau_{by}}{\rho}=0$$

$\bar{w}$ can be expressed by:

$$\bar{w}=\frac{w_b}{2}+\frac{2}{3}w_2+\frac{w_h}{2} \tag{16}$$

z-Momentum equation:

$$\frac{\partial h\bar{w}}{\partial t}+\frac{\partial hu_0\bar{w}}{\partial x}-\frac{1}{6}\frac{\partial}{\partial x}\left[hu_1(w_b-w_h)\right]+\frac{\partial hv_0\bar{w}}{\partial y}- \tag{17}$$
$$\frac{1}{6}\frac{\partial}{\partial y}\left[hv_1(w_b-w_h)\right]-\frac{1}{\rho}\frac{\partial h\bar{\tau}_{zx}}{\partial x}-\frac{1}{\rho}\frac{\partial h\bar{\tau}_{zy}}{\partial y}+$$
$$\frac{\tau_{bx}}{\rho}\frac{\partial z_b}{\partial x}+\frac{\tau_{by}}{\rho}\frac{\partial z_b}{\partial y}-\frac{p_1}{\rho}=0$$

Since the regular shallow water equations will be used for comparison the equations are given here in the nonconservative form, as they are used in the examples:

$$\frac{\partial h}{\partial t}+\frac{\partial hu}{\partial x}+\frac{\partial hv}{\partial y}=0 \tag{18}$$

$$\frac{\partial hu}{\partial t}+\frac{\partial hu^2}{\partial x}+\frac{\partial huv}{\partial y}+gh\frac{\partial(h+z_b)}{\partial x}+\frac{\tau_{bx}}{\rho}=0 \tag{19}$$

$$\frac{\partial hv}{\partial t}+\frac{\partial huv}{\partial x}+\frac{\partial hv^2}{\partial y}+gh\frac{\partial(h+z_b)}{\partial y}+\frac{\tau_{by}}{\rho}=0 \tag{20}$$

3 DERIVATION OF THE MOMENT EQUATIONS

The special weighting function

$$F=2\frac{z-\bar{z}}{h} \tag{21}$$

corresponds to the first momentum about the mid-depth point.

As an example, the derivation of the moment of continuity equation is outlined.

Integration of the continuity equation (9) using this weighting function (21) leads to

$$\int_{z_b}^{z_b+h} z\left(\frac{\partial u}{\partial x}+\frac{\partial v}{\partial y}+\frac{\partial w}{\partial z}\right)dz-\bar{z}\int_{z_b}^{z_b+h}\left(\frac{\partial u}{\partial x}+\frac{\partial v}{\partial y}+\frac{\partial w}{\partial z}\right)dz=0 \tag{22}$$

The second integral in (22) describes the mean depth multiplied with the depth averaged continuity equation. Integration by parts and the Leibniz Rule applied to the first integral term leads to:

$$\frac{\partial}{\partial x}\int_{z_b}^{z_b+h} zudz+z_bu_b\frac{\partial z_b}{\partial x}-u_h(z_b+h)\frac{\partial(z_b+h)}{\partial x}+$$
$$\frac{\partial}{\partial y}\int_{z_b}^{z_b+h} zvdz+z_bv_b\frac{\partial z_b}{\partial y}-v_h(z_b+h)\frac{\partial(z_b+h)}{\partial y}$$
$$-\bar{z}\left(\frac{\partial h}{\partial t}+\frac{\partial h\bar{u}}{\partial x}+\frac{\partial h\bar{v}}{\partial y}\right)=0$$

Depth averaging of the integral terms and introducing the kinematic conditions (7) and (8) in the previous equation, results in the final 'moment of continuity' equation:

$$\frac{\partial h\bar{z}\bar{u}}{\partial x}+\frac{\partial h\bar{z}\bar{v}}{\partial y}+(z_b+h)\frac{\partial h}{\partial t}-h\bar{w}-\left(z_b+\frac{h}{2}\right)\left(\frac{\partial h}{\partial t}+\frac{\partial h\bar{u}}{\partial x}+\frac{\partial h\bar{v}}{\partial y}\right)=$$
$$\frac{1}{4}\frac{\partial h^2}{\partial t}+\frac{1}{6}\frac{\partial h^2u_1}{\partial x}+\frac{1}{6}\frac{\partial h^2v_1}{\partial y}+hu_0\frac{\partial\bar{z}}{\partial x}+hv_0\frac{\partial\bar{z}}{\partial y}-h\bar{w}=0 \tag{23}$$

Applying the same procedure to the other Reynolds equations (10-12) gives the ensuing equations

Moment of x-momentum equation:

$$\frac{\partial u_1}{\partial t}+\frac{\partial u_0 u_1}{\partial x}+v_1\frac{\partial u_0}{\partial y}+v_0\frac{\partial u_1}{\partial y}+\frac{p_1}{2h\rho}\frac{\partial h}{\partial x}-\frac{1}{2\rho}\frac{\partial p_1}{\partial x}+$$
$$\frac{4p_2}{h\rho}\frac{\partial \bar{z}}{\partial x}-\frac{6\overline{\sigma_x}}{h\rho}\frac{\partial \bar{z}}{\partial x}-\frac{6\overline{\tau_{xy}}}{h\rho}\frac{\partial \bar{z}}{\partial y}+\frac{6\overline{\tau_{xz}}}{h\rho}+\frac{3}{h}\frac{\tau_{bx}}{\rho}=0 \quad (24)$$

Moment of y-momentum equation:

$$\frac{\partial v_1}{\partial t}+\frac{\partial v_0 v_1}{\partial y}+u_1\frac{\partial v_0}{\partial x}+u_0\frac{\partial v_1}{\partial x}+\frac{p_1}{2h\rho}\frac{\partial h}{\partial y}-\frac{1}{2\rho}\frac{\partial p_1}{\partial y}+$$
$$\frac{4p_2}{h\rho}\frac{\partial \bar{z}}{\partial y}-\frac{6\overline{\sigma_y}}{h\rho}\frac{\partial \bar{z}}{\partial y}-\frac{6\overline{\tau_{yx}}}{h\rho}\frac{\partial \bar{z}}{\partial x}+\frac{6\overline{\tau_{yz}}}{h\rho}+\frac{3}{h}\frac{\tau_{by}}{\rho}=0 \quad (25)$$

Moment of z-momentum equation:

$$\frac{\bar{w}}{4}\frac{\partial h^2}{\partial t}-\frac{\partial}{\partial t}\left[\frac{h^2}{12}(w_b-w_h)\right]-h\overline{w^2}+h\left(u_0\bar{w}-\frac{u_1}{6}(w_b-w_h)\right)\frac{\partial \bar{z}}{\partial x}$$
$$-\frac{\partial}{\partial x}\left[\frac{h^2u_0}{12}(w_b-w_h)\right]+\frac{\partial}{\partial x}\left[\frac{h^2u_1}{10}\left(\bar{w}+\frac{w_b}{3}+\frac{w_h}{3}\right)\right]$$
$$+h\left(v_0\bar{w}-\frac{v_1}{6}(w_b-w_h)\right)\frac{\partial \bar{z}}{\partial y}-\frac{\partial}{\partial y}\left[\frac{h^2v_0}{12}(w_b-w_h)\right]+ \quad (26)$$
$$\frac{\partial}{\partial y}\left[\frac{h^2v_1}{10}\left(\bar{w}+\frac{w_b}{3}+\frac{w_h}{3}\right)\right]-\frac{h}{\rho}\left(\overline{\tau_{zx}}\frac{\partial \bar{z}}{\partial x}+\overline{\tau_{zy}}\frac{\partial \bar{z}}{\partial y}-\overline{\sigma_z}\right)-$$
$$\frac{h}{2}\left(\frac{\tau_{bx}}{\rho}+\frac{\tau_{sy}}{\rho}\right)-\frac{2h}{3\rho}p_2=0$$

The mean value of the squared vertical velocity in equation 26 can be expressed by

$$\overline{w^2}=\bar{w}^2+\frac{w_b^2}{12}+\frac{w_h^2}{12}-\frac{w_b w_h}{6}+$$
$$\frac{1}{20}\left(2\bar{w}-w_b-w_h\right)^2 \quad (27)$$

4 SIMPLIFICATIONS FOR PRACTICAL USE

The vertically averaged normal and shear stresses $\overline{\sigma_x}, \overline{\sigma_y}, \overline{\sigma_z}, \overline{\tau_{xy}}, \overline{\tau_{xz}}$ and $\overline{\tau_{yz}}$ are completely neglected. For turbulent cases a closure model for the turbulence would be required.

The friction terms τ_{bx} and τ_{by} take the bed shear into account. For the following calculations the Manning-Strickler formula is used

$$\frac{\tau_{bx}}{\rho}=g\frac{u_0\sqrt{u_0^2+v_0^2+\overline{w}^2}}{k^2h^{1/3}} \quad (28)$$

where $k[\mathrm{m}^{1/3}/\mathrm{s}]$ describes the friction factor according to Strickler (k=1/n), with the Manning friction factor n. The friction could also be modeled using near bed velocities instead of the mean velocities, but for the investigated cases friction was of secondary importance. The implementation of vertical velocities is only of significance for steep slopes of the water surface. For the 1d case Khan & Steffler (1996) gave several examples using the same approach.

5 NUMERICAL MODEL

The current code is based on the FEMTOOL (Finite Element Method TOOLbox) package. This package is a general PDE solver for steady, transient, linear and nonlinear problems. It is described in more detail in Rutschmann (1993,1994). The advantage of the FEMTOOL package is the ease with which new problems can be implemented. The user has only to write the core of an element matrix routine as well as an initialization and time variation routine. For the element matrix routine this core consists of one line of code for each variable and each equation. Therefore for the standard 2D shallow water equation nine different terms have to be constructed.

FEMTOOL usually works with a standard, centered Galerkin method but uses space/time finite elements. The order of the shape functions is not limited by the package, but the order in space is decoupled from the order of approximation in time. There exists also the possibility of using different order shape functions for different variables. Also the scheme is not only capable of solving one time slab in a fully implicit way but can also solve several or all time slabs in one single fully implicit step.

For the current 2D program, linear finite elements in both, space and time, are used. On the level of the element matrix routine an upwind weighting based on the approach of Katopodes (1984) was introduced in order to reduce oscillations in the neighborhood of shocks. It has to be mentioned, that the upwind procedure is applied only to the 3 basic shallow water equations, keeping the number of additional terms as small as possible. The ten equations are simultaneously solved in nondimensional form. The nonlinearity of the equations is resolved by using Picard iteration. The convergence with this procedure is stable without any underrelaxation, although it is slow.

6 EXAMPLES

The 2-dimensional set of equations is verified for the transient dambreak problem using the same grid as Jimenez & Chaudhry (1988) and compared with the analytical solution.

The numerical simulation of supercritical flow causes several problems. Shock waves, propagating

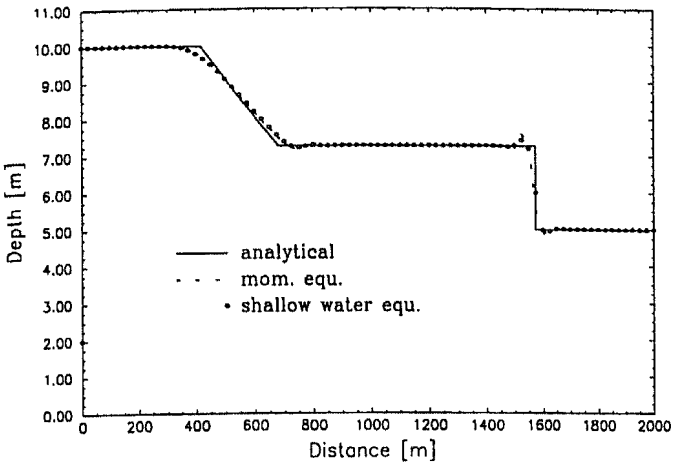

Figure 5: Water depth of a subcritical Dambreak for h/h_0 =0.5.

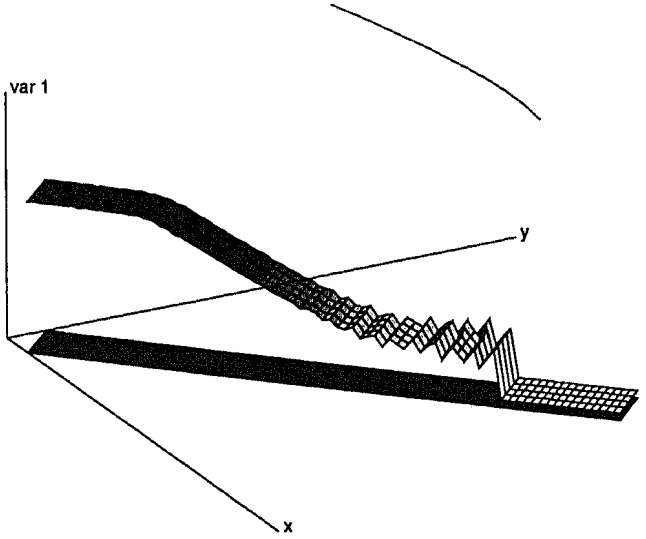

Figure 6: 3d plot of the water depth of a supercritical Dambreak for h/h_0=0.05.

from each obstacle in the channel, are difficult to handle with the FEM. Owing to the nondissipative character of the Galerkin approximation, an upwind scheme must be introduced.

6.1 Dambreak with subcritical flow

At the example of the one dimensional dambreak the comparison of the shallow water equations with the additional moment equations is demonstrated.

The problem is actually solved with the 2-d equations as given in the previous chapters, although it is basically one dimensional.

In Figure 5 the water depth of the subcritical dambreak is displayed at a time of 60 sec. after the sudden rupture. 80 linear elements of 25m length and width are used and the introduced upwind reduces spurious oscillations . The water depth ratio was set to h/h_0 =0.5, with h =10m as the initial upstream depth and h_0 the downstream depth. The difference in the depth is insignificant. The size of the other values is only shown for the supercritical dambreak flow.

6.2 Dambreak with supercritical flow

Figure 6 describes the same problem but for a water depth ratio of h/h_0 =0.05, i.e. for a supercritical dambreak. The 3d plot shows the water depth after 30 sec. No upwind is used and the grid of the 4 elements wide and 80 elements long channel lays in the diagonal, each element being 25m long and 50m wide.

Due to some difficulties with the upwind, the calculations in the diagonal direction of the coordinate system are carried out without upwind.

For the same problem in axis direction the calculations with upwind showed rather smooth results. As can be seen in Figure 7c) and e) the additional terms for the horizontal velocity u_1, resp. v_1 causes rather small deviations from the depth averaged horizontal velocity terms u_0 and v_0 in Figure 7b) and d).

The hydrostatic pressure distribution at the front where the water depth decreases suddenly from 3.1m to 0.5m, therefore is about 30 kN/m^2, resp 5 kN/m^2. Compared to those values the additional pressure terms p_1 and p_2 (Figure 7f) and g)) are small, they amount up to about 10 % of the hydrostatic pressure.

Figure 7h) to j) show the different vertical velocity terms. w_b is zero for the horizontal channel. For the depression zone, extending in both directions of the initial location of the dam at x=1000m, the vertical velocity is about -0.1 m/s, i.e. slightly negative. The zone with constant water depth between the shock front and the depression zone has a negligible vertical velocity. At the front itself the max. peak for the upwind calculation amounts up to 0.5 m/s. that means about 5-10 % of the depth averaged horizontal velocity in flow direction.

The water depth in Figure 7 a) is compared with the analytical solution of the same problem. The drag of the front of the moment equations can be ascribed to the nonconservative form of the shallow water equations that are used.

6.3 Partial Dambreak

The problem of partial dambreak as investigated by Fennema & Chaudhry (1989) and Chaudhry (1993) is solved with the moment equations.

Instead of a grid with 40 x 40 elements, as used for the original calculations, a grid with 20 x 20 linear elements is used, each element 10 by 10 m. The 200 m long and 200 m wide channel has an nonsymmetrical breach of 80 m width and 10 m

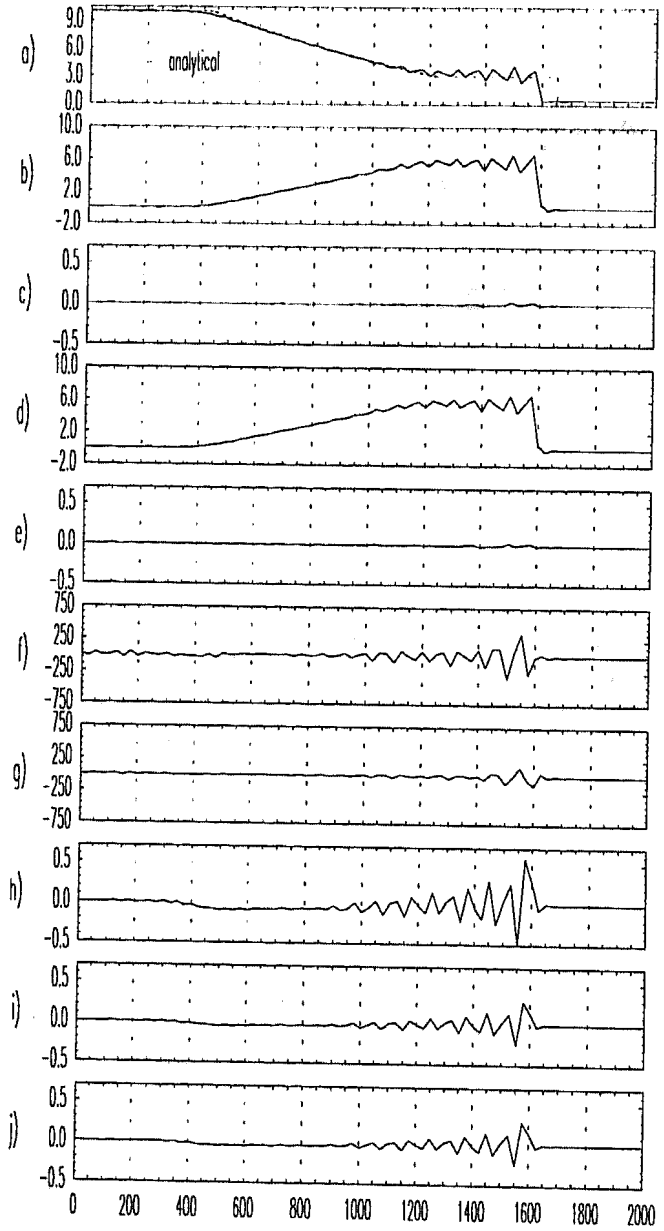

Figure 7: Graph for the 2d- dambreak with h/h_0=0.05 at t=30sec, middle slice, no upwind: a) h [m], b) u_0 [m/s], c) u_1 [m/s], d) v_0 [m/s], e) v_1 [m/s], f) p_1 [N/m^2], g) p_2 [N/m^2], h) w_h [m/s], i) $\overline{w}$ [m/s], j) w_b [m/s].

thickness. The upper border of the breach is located 30 m from the channel side. In longitudinal direction the dam is located in the middle of the channel. No upwind is introduced. No flow in and out of the calculation area is allowed. The height is nowhere cribed. For the vertical velocity and the ional pressure terms no boundary conditions are d:

uantitative analysis finer grids have to be Qualitatively the results, displayed in show that the additional equations do not ie main flow parameters. The vertical

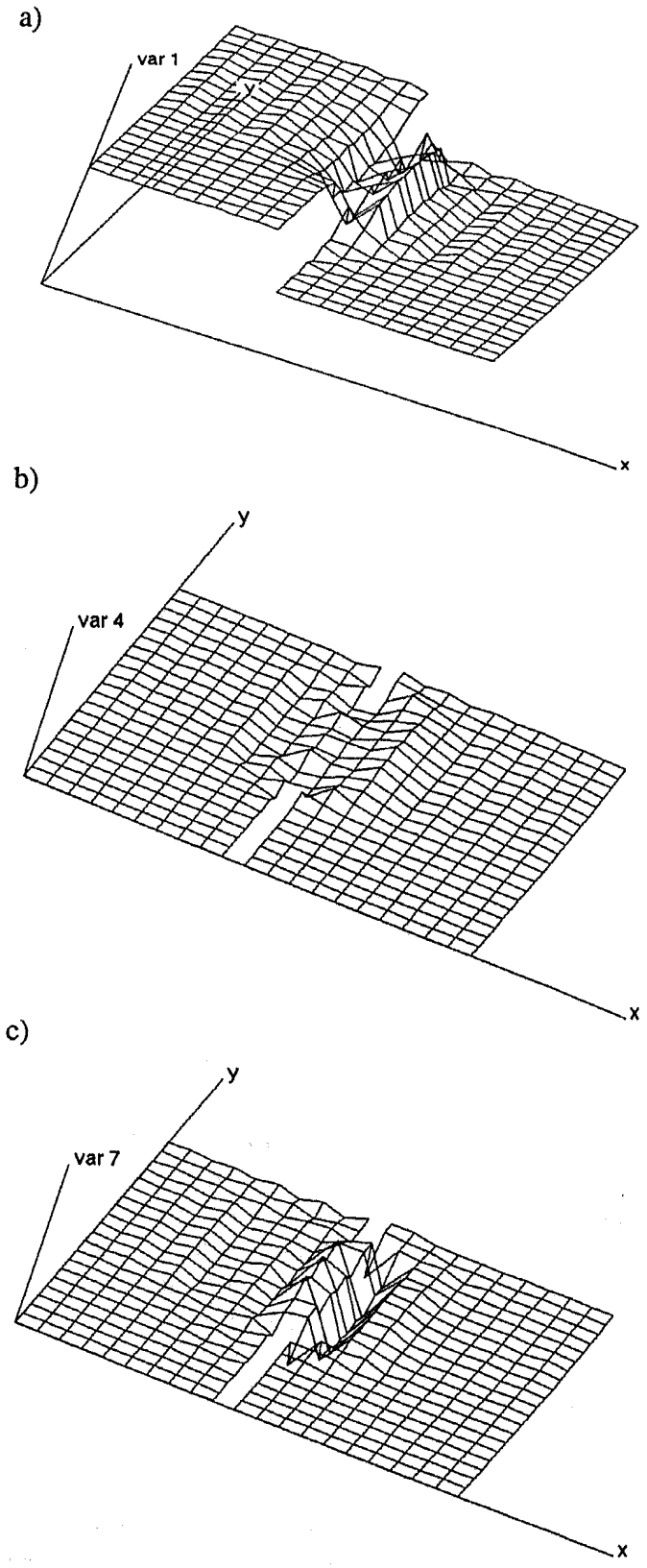

Figure 8: Partial Dambreak after 3.2 sec. a) var1=h, b) var4=w_h, c) var7=p_1.

velocity and the pressure terms only have minor influence on the solution. Locally, i.e. at locations with steep gradients in the water depth, the vertical velocity w_h amounts up to about 50 % of the horizontal velocity. The max. additional pressure p1 at the bottom is only about 15 % of the hydrostatic pressure at the same location and time.

7 CONCLUSIONS

It can be concluded, that for the overall behavior the additional terms are not of importance. But as soon as we are interested in local details, the insight given by the moment equations is tremendously deepened.

Further investigations of reasonable examples should be carried out. On the other hand measurements in the front of dambreak waves are missing. Spillway contractions or similar constructions can be easily tested with the simple 2d grid. A comparison with the general 3d Navier-Stokes equations could also be helpful.

8 ACKNOWLEDGMENTS

This research is supported by a grant of the Swiss National Science Foundation. The writer would like to thank P. Steffler for his suggestions.

REFERENCES

Chaudhry, M.H. 1993. *Open-Channel Flow.* Englewood Cliffs: Prentice Hall.

Fennema, R.J. & Chaudhry, M.H. 1989. *Journal of Hydraulic Research.* 27,3:321-332.

Jimenez, O.F. & Chaudhry, M.H. 1988. Computation of Supercritical Free-Surface Flows. *Journal of Hydraulic Engineering ASCE.* 114,4:377-395.

Katopodes, N.D. 1984. Two-Dimensional Surges and Shocks in Open Channel. *Journal of Hydraulic Engineering ASCE.* 110,6:794-812.

Khan, A.A. & Steffler, P.M. 1996. Vertically Averaged and Moment Equations Model For Flow Over Curved Beds. *Journal of Hydraulic Engineering ASCE.* 122,1:3-9.

Rutschmann, P. 1993. FE Solver with 4D Finite Elements in Space and Time. In K. Morgan, E. Oñate, J. Periaux, J. Peraire & O.C. Zienkiewicz (eds), *Finite Elements in Fluids:* 136-144. Proc. VIII. Int. Conference on Finite Elements in Fluids, Barcelona.

Rutschmann, P. 1994. Obtaining Higher Order Accuracy with Linear Shape Functions - A new approach for transient Problems. In S. Wagner, E.H. Hirschel, J. Periaux & R. Riva.(eds), *Computational Fluid Dynamics '94:* 165-169. Proc. of the Second European Computational Fluid Dynamics Conf., Stuttgart.

Steffler, P.M. & Jin, Y-C 1993. Depth Averaged and Moment Equations for Moderately Shallow Free Surface Flow. *Journal of Hydraulic Research.* 31,1:5-17.